Communications in Physics, Vol. 29, No. 4 (2019), pp. 491-500
DOI:10.15625/0868-3166/29/4/13810

TWO SPOT COUPLED RING RESONATORS

NGUYEN DUY CUONG[a,†], DINH XUAN KHOA[b], CAO LONG VAN[c], LE CANH TRUNG[b], BUI DINH THUAN[b], MAREK TRIPPENBACH[d]

[a]*Industrial University of Vinh, 26 Nguyen Thai Hoc Street, Vinh City, Vietnam*
[b]*Vinh University, 182 Le Duan Street, Vinh City, Vietnam*
[c]*University of Zielona Góra, ul. Licealna 9, 65-417 Zielona Góra, Poland*
[d]*Physics Department, University of Warsaw, ul. Pasteura 5, 02-093 Warsaw Poland.*

[†]*E-mail:* duycuonghui@gmail.com

Received 8 May 2019
Accepted for publication 28 September 2019
Published 22 October 2019

Abstract. *We consider a model of two coupled ring waveguides with a constant linear gain, a nonlinear absorption and space-dependent coupling. This system can be implemented in various physical situations as optical waveguides, atomic Bose-Einstein condensates, polarization condensates etc. It is described by two coupled nonlinear Schrödinger equations. For numerical simulations we take local two-gaussian coupling. We find that depending on the values of involved parameters, we can obtain several interesting nonlinear phenomena in the dynamics of this system, which include spontaneous symmetry breaking, modulational instability leading to generation of the stationary state periodic oscillation state, limiting cycles state, as well as dynamical regimes having signatures of chaotic behavior.*

Keywords: Bose-Einstein condensates, nonlinear optical systems, ring resonators.

Classification numbers: 42.60.-v; 42.60.Da; 67.85.Hj; 67.85.Jk.

I. INTRODUCTION

Coupled microrings are a natural laboratory studying different phenomena in both optics and Bose–Einstein condensates (BECs). In optics, they are used for nonreciprocal devices [1], switches [2], loss control of lasing [3] and ring lasers [4, 5]. Recently, the attention has also turned to more sophisticated devices, which include several coupled microcavities and are referred to as photonic molecules [6]. In the case of atomic BECs the ring-shaped geometry allows for obtaining persisting superfluid currents and considering their interaction with various types of the defects. It is reason why dynamics of atomic BECs loaded in toroidal traps have been intensively explored experimentally [7–11] and studied theoretically both in the full three-dimensional toroidal geometry [12, 13] and within the framework of the reduced quasi-one-dimensional Gross-Pitaevskii equation (GPE) with periodic boundary conditions [14–16]. Coupled non-Hermitian microcavities are also used for the study of chiral modes in exciton-polariton condensates [17] as well as for modeling coupled circular traps for BECs, which gain corresponds to adding atoms while nonlinear losses occur due to inelastic two-body interactions. Furthermore, for the cyclic geometry, many applications of the system appear due to different physical properties, for example the (cubic) nonlinearity. All considered problems are based on the same mathematical model. In optical systems, the Kerr nonlinearity is as a result of the fact that the refractive index of the medium depends on the intensity of the light, and in the mean-field theory of condensates, it appears due to two-body interactions.

In this work, we consider a model of two coupled ring waveguides with a linear gain, a nonlinear absorption and space-dependent coupling, described by two coupled nonlinear Schrödinger equations

As presented in our previous studies, the characteristics of the coupling affect the stability, as unstable modes in the dynamics are supported by the system. Dynamics depends on the geometry (i.e., on the mutual locations of the rings), on the wave-guiding characteristics of the rings, which determine the field decay outside the cavities, on the medium between the cavities (it can be homogeneous or gradient; active, absorbing or conservative), etc. Thus, it is natural interest to understand how the characteristics of coupling affect the field distribution and dynamics inside the ring cavities. This is the question addressed in the present work. For numerical simulations we take local coupling in the form of two separated Gaussians. We consider the nonlinear effects as modulational instability leading to generation of the stationary solutions, state of periodic oscillation, symmetry breaking phenomenon, limiting cycles as well as dynamical regimes having signatures of chaotic behavior in the present model will be the subjects of forthcoming papers.

Fig. 1. Schematic show of the double ring structure with linear gain γ and nonlinear loss Γ

II. THE MODEL

In the present study, we consider a model (Fig. 1) described by two coupled nonlinear Schrödinger equations with a constant linear gain and nonlinear loss (depending on the applications, they also can be termed Gross–Pitaevskii or Ginzburg–Landau equations), which we write down in scaled dimensionless units:

$$\begin{cases} i\partial_t \psi_1 = & -\partial_x^2 \psi_1 + i\gamma\psi_1 + (1-i\gamma)|\psi_1|^2\psi_1 + J(x)\psi_2 \\ i\partial_t \psi_2 = & -\partial_x^2 \psi_2 + i\gamma\psi_2 + (1-i\gamma)|\psi_2|^2\psi_2 + J(x)\psi_1 \end{cases} \tag{1}$$

Obviously, t is time, x is the angular variable varying between 0 and 2π, ψ_1 and ψ_2 are the fields in the first and second waveguides, γ is the linear gain and Γ is the nonlinear loss, both considered constants along the waveguides, and $J(x)$ is the position-dependent coupling.

Extended discussion of the model (1) and its applications can be found in a publication [18], where the rings were homogeneously coupled, i.e., where it was assumed that $J(x)$ is constant. We also mentioned that (1) with constant coupling is analogous to the model introduced earlier in [19], with local single-Gaussian coupling modulation [20], where it was considered on the whole axis subject to the zero boundary conditions. In this paper, we focus on expanding the study of the model through introducing double-Gaussian coupling modulation $J(x)$. We consider rings assuming, without loss of generality, that $x \in [-\pi, \pi]$. This implies periodic boundary conditions for both channels: $\psi_i(x,t) = \psi_i(x+2\pi,t)$, and the coupling function $J(x)$ is extended only in a certain region of the rings. In particular, for numerical simulations, we shall consider local Gaussian coupling in the following form:

$$J(x) = \frac{J_0}{\sqrt{\pi}a}\left\{\exp\left(-\frac{\left(x-\frac{\pi}{2}\right)^2}{a^2}\right) + \exp\left(-\frac{\left(x+\frac{\pi}{2}\right)^2}{a^2}\right)\right\}, \tag{2}$$

here a is the width of the coupling, while J_0 characterizes the coupling strength. Our results are not sensitive to the particular shape of the wavefunction, as we have checked using super Gaussian functions with very high power.

An important remark about the terminology used is in order. For all applications mentioned in the introduction, the meaning of the variable $x$is an angle defining a point on the circumference. The functions $\psi_{1,2}$ are envelopes of the field distributions rather than the total fields (see, e.g., [21] for optical resonators and [22, 23] for BECs applications). System (1) is simple, but possesses a surprisingly rich and diverse set of stable states (some of them nonstationary). For the limit of very wide coupling ($a \gg \pi$), we expect the same results dynamics as for the single-Gaussian coupling (this is described in [20]). On the other hand, very narrow coupling ($a \ll \pi$) allows approximating coupling with the delta function.

Most of the results found in the present study are numerical. For convenience, there is one important issue that we need to address before we present the outcome of our investigations. As discussed in [10], for the uncoupled case ($J_0 = 0$), one can find stable background solutions in the form:

$$\psi_{1,2}(t) = \sqrt{\frac{\gamma}{\Gamma}}e^{-\frac{\gamma}{\Gamma}t} \tag{3}$$

As the rings become coupled, modulation instability occurs mostly due to the interplay between linear gain and nonlinear absorption. In the case of constant coupling in [18], two distinct

classes of solutions have been found analytically: symmetric, characterized by $\psi_1 = \psi_2$, and antisymmetric. characterized by $\psi_1 = -\psi_2$. The antisymmetric solutions are always stable, and symmetric ones are usually unstable. Therefore, we decided to perform numerical studies using the symmetric state as the initial condition. This led us to a plethora of new states and attractors [18].

We found other results of many types of solutions namely antisymmetric, symmetric and asymmetric solutions. Most of the states are stationary for the width of broad coupling. For narrow coupling, the results can be stable, stationary, symmetry breaking, limit cycles or even chaotic states. Hence, we focus on the dynamics for narrow coupling. The initial state with small perturbation imposed in the form of:

$$\psi_{1,2}\,(x,t=0) = \sqrt{\frac{\gamma}{\Gamma}}\,(1+\beta\sin(kx)) \tag{4}$$

Here, the perturbation β was typically of the order of 10^{-2}. In our simulations, we took the value of the linear gain parameter γ and nonlinear loss $\Gamma = 1$ in case double-Gaussian coupling model and we checked that all results are qualitatively the same, regardless of the particular values of these parameters. All simulations were performed by two methods that are "pseudospectral method" and "Split-Step Fourier" [24]. We confirm that the results are the same for these two methods.

III. RESULTS AND DISCUSSION

III.1. Stationary Solution

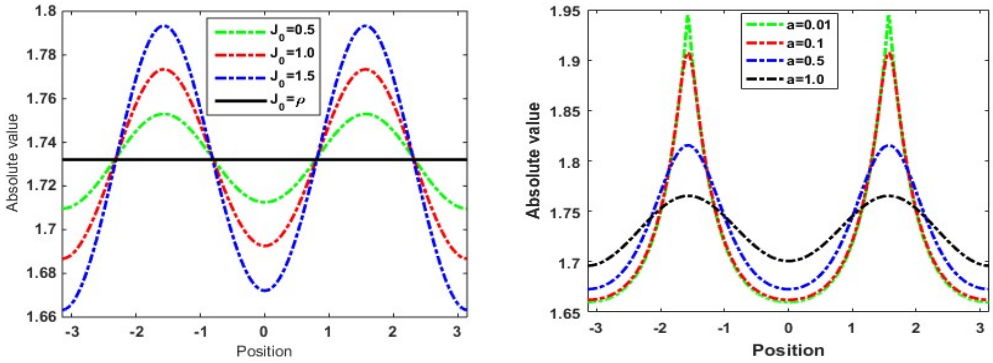

Fig. 2. Absolute values of antisymmetric stationary states after propagation time $t = 400$ in the coupled double-ring system (1) obtained for the initial conditions (4) with $\gamma = 3$ and $\Gamma = 1$. Left panel: Antisymmetric states calculated for different coupling strengths and fixed coupling width $(a = 1)$. The black line represents the homogeneous state for the respective uncoupled system. Right panel: Antisymmetric states calculated for different coupling widths and fixed normalized coupling $(J_0 = 0.8)$.

In this part, we focus on static solutions, considered the cases which are the antisymmetric, symmetric, asymmetric solutions of double-Gaussian coupling model, at the time briefly mention other cases. We obtained stationary symmetric solutions when the coupling values of J_0 are small. When the coupling between the rings is weak $(J_0 \lesssim 0.8)$ with the initial state (4), we observed that

the propagation leads to stably stationary antisymmetric solutions. These states have unchanged shape with two peaks and maximum of modulus depends on the strength of coupling J_0 (as seen in Fig. 2). In this figure, we plot the modulus of wavefunctions when the width of double-Gaussian coupling $a = 1$ and in the cases of the different strength couplings (the left panel). On the right panel, we fix the strength coupling $J_0 = 0.8$, change a direction forward to decrease the coupling which has the form of Dirac delta function. Also, we show background level, plotting it as a black horizontal reference line.

We compare these results with the previous results of the article [20]. The similarity is that there is the decrease of modulus of wavefunction at $x = \pm\pi$ when we increase the ratio strength coupling J_0/a. The difference is that in our model minimum modulus of wavefunction has the value at $x = \pm x_m$ for all values of J_0 while in the paper [20] the minimum modulus of wavefunction is achieved at value $x = \pm x_m$ with $x_m =\leq \pi$.

In the following sections, we will present dynamics of the system when the strength coupling is tuned up. We divided the description into two strength coupling regimes which are narrow $(a \ll 1)$ and extended $(a \geq 1)$) width coupling.

III.2. Narrow Coupling Dynamics

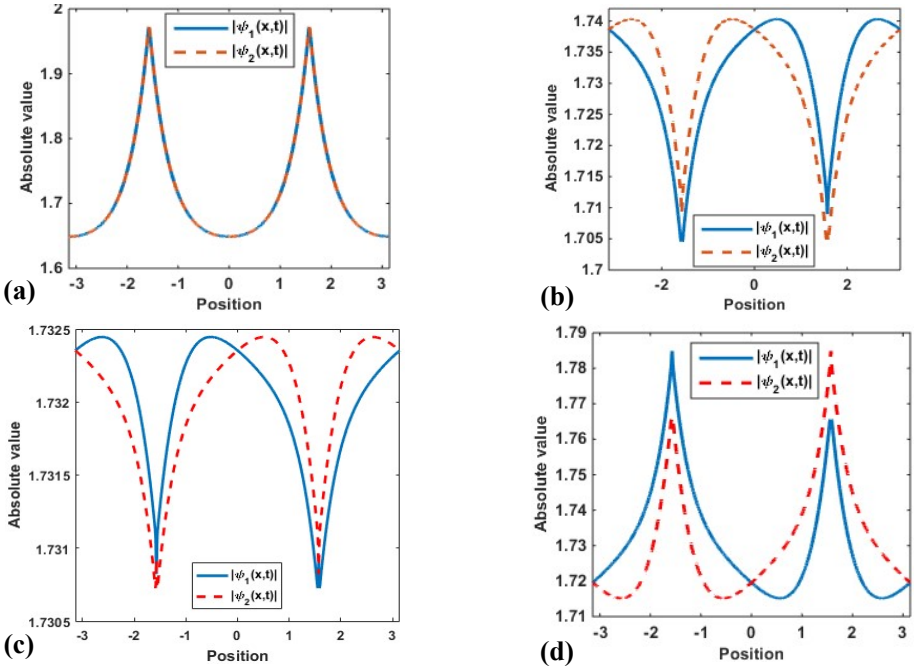

Fig. 3. Absolute value of the wavefunctions in the case $\gamma = 3$, $\Gamma = 1$ and $\alpha = 0.01$. Parameters are (a) $J_0 = 0.9$; (b) $J_0 = 0.95$; (c) $J_0 = 1.0$ and (d) $J_0 = 1.1$.

In this section, we considered the double-Gaussian coupling model with narrow width of coupling strength $J(x)$ (see formula (2), we used $a = 0.01$). The results were summarized in Figures 3, 4 and 5. With growing values of the coupling strength J_0, we obtained results that

represent stationary states, cyclic states, symmetry breaking, chaotic phenomenon. The quantity used by us to characterize different kinds of possible states is a total norm defined as:

$$N(t) = \int_{-\pi}^{\pi} \left[|\psi_1(x,t)|^2 + |\psi_2(x,t)|^2 \right] dx. \tag{5}$$

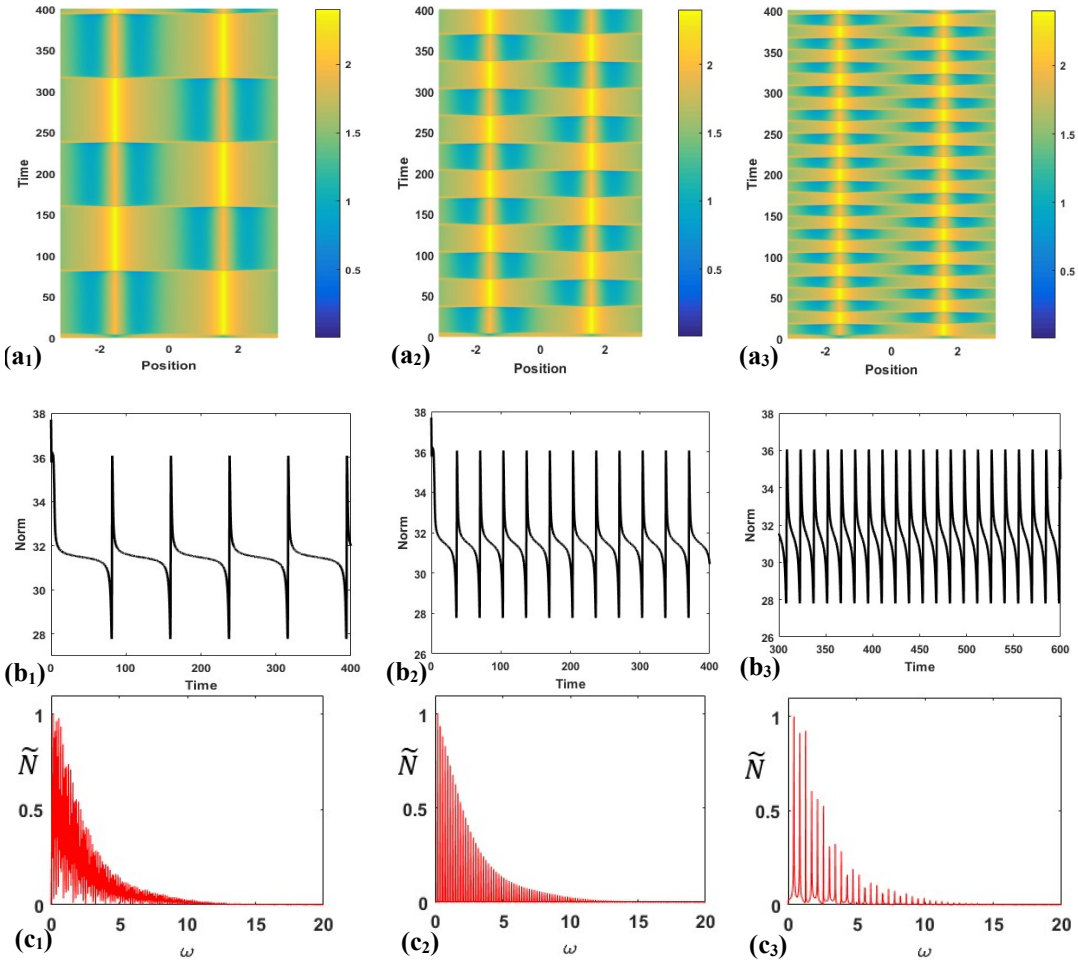

Fig. 4. Top row shows contour plots of absolute values of the propagated wavefunction ψ_1 in the stationary (asymptotic) regime (panels (a_1, a_2, a_3)), center row presents total norm as a function of time, bottom row shows normalized modulus of Fourier transform of the total norm defined in Eq. (5) for three different coupling strengths J_0 and the fixed width $a = 0.01$ ((a_1-c_1), (a_2-c_2), (a_3-c_3) corresponding with $J_0 = 2.598$, $J_0 = 2.600$, $J_0 = 2.610$).

For small coupling $J_0 \lesssim 0.8$, we always obtained stable stationary states for anti-symmetric. When $J_0 \approx 0.95$, the simulation results that there is symmetry breaking in each channel. As in Fig. 3b, we see that the dashed red and solid blue lines have asymmetry through vertical axis passing the point 0. This symmetry breaking in each channel occurs until the coupling value $J_0 = 3.2$.

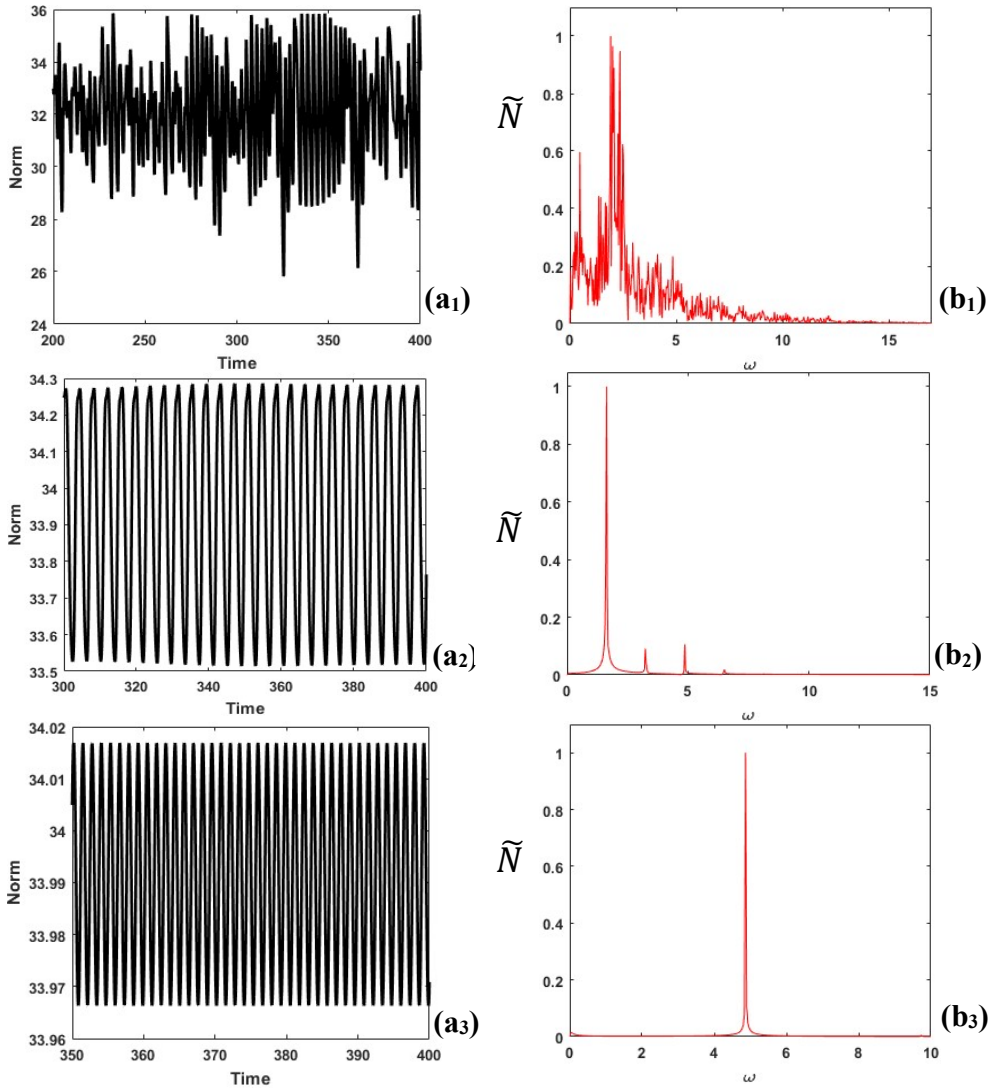

Fig. 5. Total norm as a function of time is shown in the left column (figures (a_1, a_2, a_3)). The right column presents normalized modulus of Fourier transform of the total norm defined in Eq. (5) for three different coupling strengths J_0 and the fixed width $a = 0.01$ ((a_1-b_1), (a_2-b_2), (a_3-b_3) corresponding with $J_0 = 2.84$, $J_0 = 3.19$, $J_0 = 3.20$).

Asymmetric states maintain when the strength coupling varies in the range of $J_0 : 0.95 \lesssim J_0 \lesssim 2.597$. However, in the process of increasing J_0 in that range, we also observe changing state from dark to bright at $J_0 = 1.1$.

Figure 4 represents graphically typical situations found for a long time dynamics of the system. We observe an oscillatory behavior and, with $2.598 \lesssim J_0 \lesssim 2.61$, our system tends to the complex oscillation, and we observe oscillations symmetric with respect to the center of the coupling region. At the same time, if the coupling strength increases then oscillation frequency

will go up. In bottom row, normalized modulus of Fourier transform of the total norm defined in Eq. (5) for three different coupling strengths $J_0 = 2.598$, $J_0 = 2.600$, $J_0 = 2.610$ are shown, in which order the complexity of the oscillation decreases and the antisymmetric stationary state is turned on again at $J_0 = 2.62$.

Moving to the next process, when $2.62 \lesssim J_0 \lesssim 2.83$ then anti-symmetric stationary states appear again, when $2.84 \lesssim J_0 \lesssim 3.17$ the chaos behavior phenomenon appears and when $3.18 \lesssim J_0 \lesssim 3.2$ chaos ends up abruptly and oscillation states appear again. Fig. 5 shows three cases of the coupling strength J_0 which represent three characteristic types of oscillation. Figures $5a_1$ and $5b_1$ present route to chaos, figures $5a_2$ and $5b_2$ present the dynamics of the system becoming more complicated and the modulus of Fourier transform oscillating with different periods. In figures $5a_3$ and $5b_3$ we observe simple regular oscillations with the modulus of Fourier transform oscillating only with single frequency. Before the dark-symmetry states appears at the coupling strength $J_0 \gtrsim 3.4$, the dark-asymmetry state arises already at $J_0 = 3.3$.

III.3. Broad Coupling Dynamics

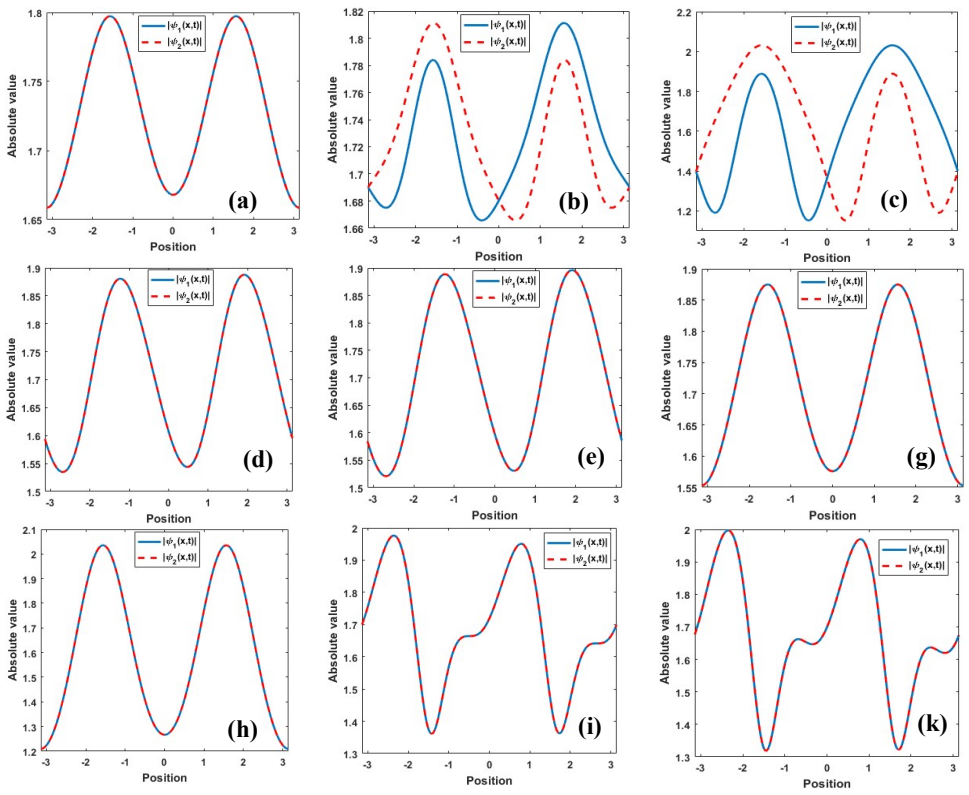

Fig. 6. The absolute values of the propagated wavefunction in the stationary (asymptotic) regime for three different coupling strengths J_0 and the fixed width $a = 1$, at the time $t = 400$, ((a), (b), (c), (d), (e), (g), (h), (i), (k) corresponding with $J_0 = 1.6$, $J_0 = 1.7$, $J_0 = 3.3$, $J_0 = 3.4$, $J_0 = 3.6$, $J_0 = 3.7$, $J_0 = 9.4$, $J_0 = 9.5$, $J_0 = 10.5$).

When the coupling width is broad, it means that it is comparable to the length of the ring we also observed a few classes of characteristic steady state dynamics, when the value of coupling strength J_0 increases. If the coupling strength $J_0 \lesssim 1.6$ or $3.7 \lesssim J_0 \lesssim 3.94$, the state dynamics will always leads to the stationary anti-symmetric solutions. The asymmetric states appear when $1.7 \lesssim J_0 \lesssim 3.3$ then we have symmetry breaking in each ring. The anti-symmetric solutions and symmetry breaking in each ring occur in the range of J_0 are $3.4 \lesssim J_0 \lesssim 3.6$ and $9.5 \lesssim J_0 \lesssim 10.5$.

Now we continue to increase the intensity of the coupling, the chaotic behavior appears at $J_0 = 10.8$, the chaotic state exists when $J_0 \gtrsim 14$, and in a small interval from $J_0 \simeq 12.6$ to $J_0 \simeq 12.9$. The complex oscillation state exists when J_0 changes from 11 to 12.6 and from 12.9 to 14.

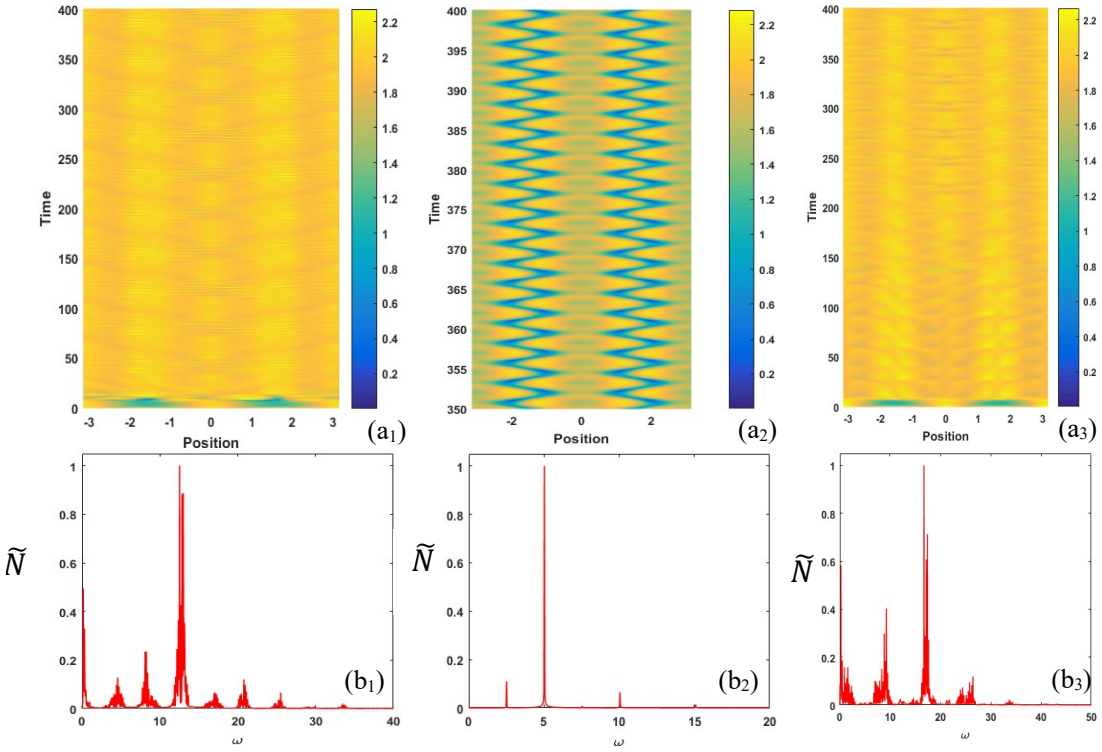

Fig. 7. Upper row presents contour plots of absolute values of the propagated wavefunction ψ_1 in the oscillations regime for three different coupling strengths J_0 and the fixed width $a = 1$. Bottom row shows normalized modulus of Fourier transform of the total norm defined in Eq. (5). Panels (a_1, b_1), (a_2, b_2), (a_3, b_3) corresponding with $J_0 = 10.7$, $J_0 = 12$, $J_0 = 13.95$.

IV. CONCLUSION

In this work, we have studied the model of two coupled rings, described by nonlinear Schrödinger equations with a linear gain and a nonlinear loss and the coupling in the form of double-Gaussian. Such a system may physically correspond to models of microresonator nanostructures, polariton condensates or coupled optical waveguides. We have identified stationary and

dynamic solutions both in the case of narrow and broad coupling by changing one control parameter that is the coupling strength. As we adjusted the value of the coupling strength from small to large values, the stationary solutions, oscillatory solutions, symmetry breaking phenomenon, limiting cycles, chaotic behavior were observed.

ACKNOWLEDGMENTS

This research is funded by Vietnam's Ministry of Science and Technology (ĐTĐL.CN-32/19).

REFERENCES

[1] B. Peng, S. K. Özdemir, F. Lei, F. Monifi, M. Gianfreda, G. Lu, L.G. Long, S. Fan, F. Nori, C. M. Bender, et al, *Nat. Phys.* **10** (2014) 394.
[2] L. Chang, X. Jiang, S. Hua, C. Yang, J. Wen, L. Jiang, G. Li, G. Wang, M. Xiao, *Nat. Photon.* **8** (2014) 524.
[3] B. Peng, S. K. Özdemir, S. Rotter, H. Yilmaz, M. Liertzer, F. Monifi, C. M. Bender, F. Nori, L. Yang, *Science* **346** (2014) 328.
[4] M. Liertzer, L. Ge, A. Cerjan, A. D. Stone, H. E. Tuüreci, S. Rotter, *Phys. Rev. Lett.* **108** (2012) 173901.
[5] H. Hodaei, M. A. Miri, M. Heinrich, D. N. Christodoulides, M. Khajavikhan, *Science* **346** (2014) 975.
[6] Y. Li, F. Abolmaali, K. W. Allen, N. I. Limberopoulos, A. Urbas, Y. Rakovich, A. V. Maslov and V. N. Astratov, *Phys. Rev. Lett.* **11** (2017) 1600278.
[7] C. Ryu, et al, *Phys. Rev. Lett.* **99** (2007) 260401.
[8] C. N. Weiler, et al, *Nature London.* **455** (2008) 948.
[9] K. Henderson, C. Ryu, C. MacCormick and M. G. Boshier, *New J. Phys.* **11** (2009) 043030.
[10] B. Murphy, et al, *Phys. Rev. Lett.* **106** (2011) 130401.
[11] S. Eckel, et al, *Nature* **506** (2014) 200.
[12] S. Komineas and J. Brand, *Phys. Rev. Lett.* **95** (2005) 110401.
[13] P. L. Halkyard, M. P. A. Jones and S. A. Gardiner, *Phys. Rev. A* **81** (2010) 061602.
[14] G. P. Agrawal, *Non linear Fiber optics* Academic Press: San Diego, CA, USA, 2001, ISBN 0-12-045143-3.
[15] A. Kosiorek, W. Kandulski, P. Chudzinski, K. Kempa, M. Giersig, *Nano Lett.* **47** (2004) 1359.
[16] H. Saito and M. Ueda, *Phys. Rev. Lett.* **93** (2004) 220402.
[17] T. Gao, G. Li, E. Estrecho, T. C.H. Liew, D. Comber-Todd, A. Nalitov, M. Steger, K. West, L. Pfeiffer, D. W. Snoke, A. V. Kavokin, A. G. Truscott and E. A. Ostrovskaya, *Phys. Rev. Lett.* **120** (2018) 065301.
[18] N. V. Hung, K. B. Zegadlo, A. Ramaniuk, V. V. Konotop, M. Trippenbach, *Sci. Rep.* **7** (2017) 4089.
[19] A. Sigler and B. A. Malomed, *Phys. D Nonlinear Phenom.* **212** (2005) 305.
[20] A. Ramaniuk, N. V. Hung, M. Giersig, K. Kempa, V. V. Konotop and M. Trippenbach, *Symmetry* **10** (2018) 195.
[21] Y. K. Chembo, C. R. Menyuk, *Phys. Rev. A* **87** (2013) 053852.
[22] H. Saito and M. Ueda, *Phys. Rev. Lett.* **93** (2004) 220402.
[23] Y. V. Bludov, V. V. Konotop, *Phys. Rev. A* **75** (2007) 053614.
[24] J. Yang, *Monographs on Mathematical Modeling and Computation*, Society for Industrial & Applied Mathematics, U.S., 2010.